1

E3 Ligase UBR5 HECT domain mutations in lymphoma control maturation of B cells via alternative splicing

Samantha A. Swenson[1,2,7], Tyler J. Gilbreath[1,2,7], Heather Vahle[1,2], R. Willow Hynes-Smith[1,2], Jared H. Graham[1], Henry Chun Hin Law[2,3], Nicholas T. Woods[2,3], Michael R. Green[4,5,6] and Shannon M. Buckley[1,2,*]

[1]Department of Genetics, Cell Biology, and Anatomy, University of Nebraska Medical Center, Omaha, NE, USA; [2]Fred and Pamela Buffet Cancer Center, University of Nebraska Medical Center, Omaha, NE, USA; [3]Eppley Institute, University of Nebraska Medical Center, Omaha, Nebraska, USA; [4]Department of Lymphoma and Myeloma, Division of Cancer Medicine, The University of Texas MD Anderson Cancer Center, Houston, TX, USA; [5]Department of Genomic Medicine, University of Texas MD Anderson Cancer Center, Houston, TX, USA; [6]Center for Cancer Epigenetics, University of Texas MD Anderson Cancer Center, Houston, TX, USA.; [7]These authors contributed equally to this study

RUNNING TITLE – UBR5 HECT domain mutations in B cell development

*Address Correspondence To:

Shannon M. Buckley, Ph.D.
Department of Genetics, Cell Biology, and Anatomy
University of Nebraska Medical Center
985805 Nebraska Medical Center
Omaha, NE 68198
Email: Shannon.Buckley@unmc.edu

Word Counts:

Abstract: 194, Text: 3,968, Figures: 7, References: 38

Scientific category: Immunobiology and Lymphoid Neoplasms

KEY POINTS

- Utilizing a novel mouse model mimicking MCL patient mutations, the loss of UBR5's HECT domain causes alterations in B cell development.

- UBR5 mutations lead to stabilization of UBR5 and aberrant splicing.

ABSTRACT

Coordination of a number of molecular mechanisms including transcription, alternative splicing, and class switch recombination are required to facilitate development, activation, and survival of B cells. Disruption of these pathways can result in malignant transformation. Recently, next generation sequencing has identified a number of novel mutations in mantle cell lymphoma (MCL) patients including the ubiquitin E3 ligase UBR5. Approximately 18% of MCL patients were found to have mutations in UBR5 with the majority of mutations within the HECT domain of the protein which can accept and transfer ubiquitin molecules to the substrate. Determining if UBR5 controls the maturation of B cells is important to fully understand malignant transformation to MCL. To elucidate the role of UBR5 in B cell maturation and activation we generated a conditional mutant disrupting UBR5's C-terminal HECT domain. Loss of the UBR5 HECT domain leads to a block in maturation of B cells in the spleen and up-regulation of proteins associated with mRNA splicing via the spliceosome. Our studies reveal a novel role of UBR5 in B cell maturation by regulating alternative splicing of key transcripts during B cell development and suggests UBR5 mutations may promote mantle cell lymphoma initiation.

INTRODUCTION

Mantle Cell Lymphoma (MCL) is a rare, aggressive form of Non-Hodgkin's Lymphoma (NHL).[1] Although MCL represents only ~6% of NHL lymphoma cases, it has one of the highest mortality rates of all lymphomas with only a 50% five year survival.[2] Given the high mortality rate and propensity for recurrence, having better comprehension of mutations found in MCL and how disease develops in B cells will open avenues for identifying new therapies. Recently, the ubiquitin protein ligase E3 component n-recognin 5 (UBR5) was found mutated in ~18% of patients with MCL.[3] The majority of mutations identified in *UBR5* were frame shift mutations found within its HECT domain, which can accept and transfer ubiquitin molecules to the substrate, leading to a premature stop codon prior to the cysteine residue associated with ubiquitin transfer.

UBR5 is a large ~300kDa protein HECT E3 ligase with a conserved carboxyl-terminal HECT domain. In HECT E3 ligases, the N-terminal portion (N-lobe) of the enzyme interacts with E2 ubiquitin-conjugating enzymes and determines substrate specificity while the C-terminal HECT domain (C-lobe) contains a catalytic cysteine residue that binds ubiquitin.[4] The two lobes are connected by a flexible linker that allows for shifting orientation between N- and C-lobes during ubiquitin transfer to allow for efficient movement of ubiquitin from the E3 ligase to the substrate protein. UBR5 regulates a number of cellular processes including metabolism, apoptosis, angiogenesis, gene expression, and genome integrity.[5-10] Overexpression of UBR5 has been found in a number of cancers including ovarian, breast, hepatocellular, squamous cell carcinoma, and melanoma.[11-14]

3

77   Determining if, and at what stage – transcriptional, translational, or proteomic – UBR5

78   controls maturation of B cells is important for fully understanding B cell development and

79   lymphoma transformation. In order to elucidate the role of UBR5 in B cell maturation and

80   activation, we generated a conditional mutant disrupting the C-terminal HECT domain. Loss of

81   the HECT domain leads to a block in maturation of B cells, and follicular B cells are

82   phenotypically abnormal with low expression of IgD and high expression of IgM. Upon immune

83   stimulation, B cells lacking the HECT domain show decreased germinal center formation and

84   reduced antibody producing plasma cells suggesting both defects in phenotype and function

85   of mature B cells. Proteomic studies reveal up-regulation of proteins associated with mRNA

86   splicing via the spliceosome and indicates that UBR5 interacts with splicing factors (SF3B3,

87   SMC2, PRPF8, DHX15, SNRNP200, and EFTUD2). Our studies reveal a novel role of UBR5

88   in B cell maturation by regulating alternative splicing of key transcripts during B cell

89   development and suggests *UBR5* mutations in MCL lead to disease initiation.

90

91   **METHODS**

92   **Mice**

93   *Ubr5* HECT mutant mice were developed using Easi-CRISPR as previously published[15]

94   and crossed with *Mb1*[CRE] mice (kind gift of Michael Reth). Floxed *Ubr5* alleles were validated

95   by PCR using primers designed to amplify targeted alleles (supplemental materials and

96   methods). For immune stimulation, mice were immunized by intraperitoneal injection with

97   1×10^8 sheep's red blood cells (SRBC) (Innovative Research). All mice were housed in a

98   pathogen-free facility at University of Nebraska Medical Center. Procedures performed were

99 approved by Institutional Animal Care and Use Committee of University of Nebraska Medical

100 Center in accordance with NIH guidelines.

101

102 **B cell isolation and culture**

103 Total bone marrow (BM) and splenocytes were isolated from 6-week-old mice. B220^{+} cells

104 were isolated using MojoSort Streptavidin Nanobeads (Biolegend, San Diego, CA) following

105 manufacturer's protocol. B cells were cultured in RPMI 1640 Base Media (Hyclone), 10% fetal

106 bovine serum (Atlanta Biologicals), 2mM L-glutamine (Corning), 50µM 2-mercaptoethanol

107 (Corning), 20mM HEPES (4-(2-hydroxyethyl)-1-piperazineethanesulfonic acid) (Hyclone), and 1X

108 penicillin/streptomycin. Cycloheximide (Millipore) was used at a final concentration of 10µg/mL.

109

110 **FlowCytometry analysis**

111 For flowcytometry analysis cells were stained for 1 hour in 3% FBS in PBS. Antibodies found

112 in supplemental materials and methods. For cell cycle analysis, cells were fixed and permeabilized

113 following Biolegend intracellular staining protocol and stained with Ki67 and DAPI (4',6-diamidino-

114 2-phenylindole).

115

116 **ELISA**

117 Mice were bled on Day 0 and Day 8 following immune stimulation. Serum was collected

118 following Abcam ELISA sample preparation guide, diluted 1:10 with PBS. SRBC, diluted 1:10 in

119 PBS, was used as a control for cross reactivity of antibodies due to presence of SRBC. ELISA was

120 performed with positive reference antigen mixture, and PBS as a negative control according to

121 manufactures directions (BD Pharmingen).

122

Histological Staining

Mouse spleens were fixed in 10% (vol/vol) buffered formalin phosphate for 24 hours then placed in 70% ethanol. Sections were stained with H&E using standard protocols. Spleen sections were stained in a 1:500 dilution of UBR5 antibody ab70311 (Abcam) and Ki67. For germinal center analysis, mice were immunized with SRBC and sacrificed eight days later. Spleen sections were stained in a 1:500 dilution of biotinylated peanut agglutinin (PNA) antibody B-1075 (Vector Labs). Images were captured with a Zeiss Observer.Z1 microscope (Zeiss International, Germany) and Zen Pro software (Zeiss International, Germany) was used to process the images.

131

Nuclear Fractionation

Nuclei from 293Ts (ATCC) were collected as described previously.[16] Nuclei were lysed in low salt buffer (10mM Tris-HCl pH7.4, 0.2mM $MgCl_2$, 1% Triton-X 100) containing protease and phosphatase inhibitors for 15 minutes on a rocker at 4°C. 10-30% glycerol gradients were prepared as previously described.[17] Samples were spun at 28,000rpm for 13 hours at 4°C. 200uL fractions were collected for a total of 25 fractions.

138

Western Blot and Immunoprecipitation Analysis

For western blot analysis, samples were lysed in Pierce RIPA buffer containing protease and phosphatase inhibitor cocktail (ThermoFisher). Samples were separated by SDS-PAGE, transferred onto PVDF (Millipore), and blocked in 5% milk. Antibodies were prepared in 5% BSA. Horse Radish Peroxidase conjugated secondary antibodies (Jackson laboratories) were prepared in 5% milk.

6

145

RNA extraction and quantitative real-time PCR

Total RNA was harvested using QIAGEN RNeasy Kit (QIAGEN, Hilden, Germany). Following RNA extraction, cDNA synthesis was performed using High Capacity RNA-to-cDNA Kit (ThermoFisher). qRT-PCR was carried out on equal concentrations of cDNA for each sample using iTaq Universal SYBR Green Supermix. All primers can be found in supplemental materials and methods.

Mass Spectrometry

For global proteome quantification, B220$^+$ splenocytes were isolated from 3 mice per genotype. Samples were prepared for and TMT labeled per manufacturer's protocol (ThermoScientific TMT10plex Mass Tag Labeling Kits). Following TMT labeling, acetonitrile was removed by speedvac and samples were resuspended in 0.1% trifluoroacetic acid (TFA). Sample cleanup with C18 tips was performed per manufacturer's protocol (Pierce). Sample concentrations were re-quantified (Pierce Quantitative Colorimetric Peptide Assay kit) and then combined in equal concentration. Following combination, samples were dried by speedvac and fractionated by ThermoScientific high pH reverse phase fractionation kit following manufacturer's protocol for TMT. Resulting fractions were run in a speedvac to dryness and resuspended in 0.1% Formic Acid for mass spectrometry (MS) analysis (see supplemental methods). Data are available via ProteomeXchange with identifier PXD014307.

For immunoprecipitation, cells were lysed in 20mM Tris pH 7.5, 150mM NaCl, 1mM EDTA, and protease and phosphatase inhibitors. Immunoprecipitation was performed

7

168   overnight at 4°C using anti-UBR5 antibody from Cell Signaling (8755) or rabbit IgG control.

169   Protein A agarose beads (Cell signaling) were used for IgG pulldown. Samples were washed

170   5X with lysis buffer prior to analysis by MS.

171

172   **Statistical analysis**

173   All experiments were performed in triplicate unless noted and statistical analyses were performed

174   using paired two-tailed Student's t-test assuming experimental samples of equal variance. * P<0.05,

175   ** P<0.01, *** P<0.001, **** P<0.0001

176
177
178
179   **RESULTS**
180

181   ***Ubr5* mutations are specific to MCL.**

182   Meissner, B. et al originally identified UBR5 mutations in ~18% of MCL patients.[3] In recent

183   cross-sectional genomic profiling of multiple lymphoma subtypes, we identified UBR5 as one of 8

184   genes that had a significantly higher frequency of mutation in MCL compared to other lymphoma

185   subtypes. These mutations were observed in 21 out of 196 MCL tumors (10.7%) and 15 out of 559

186   tumors (2.7%) of other histologic subtypes. However, mutations within the HECT domain were found

187   only in MCL tumors (Figure 1B).[18] Mutations within the HECT domain of UBR5 are therefore a

188   disease-specific genetic feature of MCL.

189

190   **Generation of a conditional UBR5 HECT domain mutant.**

191   Since the role of *Ubr5* in lymphopoiesis is unknown, we first evaluated the expression of *Ubr5*

192   in B cell sub-groups during development by purifying pro, pre, and immature B cells from BM of 6-

193   week-old C57/BL6 wild-type (WT) mice. Additionally, transitional, follicular, and marginal zone B cell

194   populations were purified from spleens. The pro B cell population showed lowest expression of *Ubr5*

195   at both the RNA and protein level, whereas the highest expression of *Ubr5* was found in mature

196   splenic populations (follicular and marginal B cells) (Figure 1B-C). These studies suggest a role for

197   UBR5 at different stages of B cell development.

198

199   Saunders *et al.* generated a *Ubr5*-null mouse; unfortunately, these mice die during

200   embryogenesis prior to onset of definitive hematopoiesis at E10.5.[19] In order to understand the role

201   of UBR5 mutations in B cell development, we generated a conditional allele targeting exon 58 that

202   would lead to a truncated protein lacking a critical cysteine required for ubiquitin conjugation in the

203   HECT domain and mimicking mutations found in MCL patients (Figure 1D).[20] We first crossed our

204   *Ubr5$^{\Delta HECT/+}$* mice to *E2A^{CRE};Ubr5$^{\Delta HECT/+}$* mice that delete in early embryogenesis.[19, 21] As with null

205   mice, *E2A^{CRE};Ubr5$^{\Delta HECT/\Delta HECT}$* were not viable. In contrast to *Ubr5*-null mice, 3 of 48 pups found dead

206   at birth were *E2A^{CRE};Ubr5$^{\Delta HECT/\Delta HECT}$,* suggesting the HECT domain is not required for embryogenesis

207   and early stages of hematopoiesis (Figure 1E-F).

208

209   Since *E2A^{CRE};Ubr5$^{\Delta HECT/\Delta HECT}$* mice die prior to or at birth, to study B cell development we

210   crossed *Ubr5$^{\Delta HECT/\Delta HECT}$* mice to *Mb1$^{WT/CRE;}$ Ubr5$^{\Delta HECT/\Delta HECT}$*, which deletes in early B-lymphocytes

211   (Figure 1G).[22] To determine the specific loss of the HECT domain, we performed qRT-PCR with

212   primers flanking the HECT domain and primers amplifying a region on the N-terminus in B220$^+$

213   splenocytes. qRT-PCR showed no decrease in *Ubr5* expression, but significant decrease in *Ubr5*

214   HECT domain expression (Figure 1H). These studies demonstrate the loss of HECT domain of UBR5

215   targeted mice.

216

Impaired B cell maturation following deletion of UBR5 HECT domain..

Early B cell development occurs in the BM compartment so we examined BM B cells in 6-week-old $Mb1^{WT/CRE}$;$Ubr5^{\Delta HECT/\Delta HECT}$ mice. In $Ubr5^{\Delta HECT/\Delta HECT}$ and $Ubr5^{\Delta HECT/WT}$ mice, the number of total BM cells and frequency of B220$^+$ B cells showed no significant difference compared to their WT littermates (Figure 2A-C; Supplemental Figure 1A-B). Further analysis of specific subtypes of B cells revealed a striking decrease in IgD$^+$ mature B cell populations (Figure 2D-E; Supplemental Figure 1C-D). Decreases in mature B cells were compensated in BM by a slight increase in propre B cell population (Figure 2F-G). Further breakdown of the population revealed an increase in pro B, but not pre B cell population (Figure 2F-I). These studies demonstrate an impact to mature cells within BM, as well as changes to composition of pro and pre B cells following loss of HECT domain.

Following development of B cells in BM, cells migrate to the spleen where they undergo maturation and activation.[23] $Mb1^{CRE/WT}$;$Ubr5^{\Delta HECT/\Delta HECT}$ mice have smaller spleens as well as a reduction in number of total splenocytes (Figure 3A-B). Although the mice had a total reduction of splenocytes, frequency of B220$^+$ cells in both WT littermates and $Ubr5^{\Delta HECT/\Delta HECT}$ mice was ~45% (Figure 3C), and splenic architecture was unaltered following loss of the HECT domain of $Ubr5$ (Figure 3D). In addition, the transitional B cell population stages T1, T2, and T3 in the spleen had no significant differences in $Ubr5^{\Delta HECT/\Delta HECT}$ mice versus WT littermates (Figure 3 E-F). However, there was significant impact on mature B1 and B2 subsets within the spleen. We found that in the B2 subset, marginal zone B cells were significantly reduced from approximately 10% of B220$^+$ splenocytes to 2% in $Ubr5^{\Delta HECT/\Delta HECT}$ mice whereas the follicular B cell compartment frequency was slightly

10

238 increased, despite a reduction in absolute number of follicular B cells in $Ubr5^{\Delta HECT/\Delta HECT}$ mice (Figure

239 3H-I; Supplemental Figure 1E-F).

240

241   The B1 population is responsible for innate immunity and is the first line of defense for infection.

242 In spleen, the B1 population was reduced by almost 2-fold in $Ubr5^{\Delta HECT/\Delta HECT}$ mice and when further

243 separated into B1a and B1b, the reduction was exclusively found in the B1a subpopulation (Figure

244 3K-M). We further evaluated B1 populations in the peritoneal cavity and found a ~75% reduction in

245 B1 cells, mainly from a reduction of B1a cells (Supplemental Figure 2). These findings demonstrate

246 a significant loss of populations required for innate immunity with loss of B1 and marginal zone B cells

247 following deletion of the HECT domain of $Ubr5$.

248

249 **Alterations in follicular B cell subsets and activation of B cells.**

250   Evaluating cell surface markers on the follicular B cell population, we found that

251 $Ubr5^{\Delta HECT/\Delta HECT}$ follicular B cells had abnormal protein expression with low IgD and high IgM

252 compared to their WT littermates (Figure 4A-B). The follicular population in $Ubr5^{\Delta HECT/\Delta HECT}$ mice also

253 had high CD23 protein expression, but normal expression of CD5 and CD1d on follicular B cells

254 (Figure 4A-B). To further define alterations in the B cell compartment, we analyzed cell cycle status.

255 While follicular B cells are typically in the resting state, $Ubr5^{\Delta HECT/\Delta HECT}$ cells are more quiescent and

256 had increased cells in G0 for both transitional and mature B cells (Supplemental Figure 3A).

257 Additionally, staining with cellular proliferation marker Ki67 on spleen sections showed a reduction of

258 Ki67 staining specifically in white pulp of spleens from $Ubr5^{\Delta HECT/\Delta HECT}$ mice (Supplemental Figure

259 3B). These studies demonstrated alterations in mature spleen cells with both phenotypic changes

260 and cell cycle alterations.

261

262   Activation of follicular B cells by T dependent antigens leads to formation of germinal centers

263 (GC) in secondary lymphoid tissues and generation of antibody producing plasma cells. In order to

264 determine if $Ubr5^{\Delta HECT/\Delta HECT}$ follicular B cells have normal function and whether germinal center

265 formation can be induced, we immunized 6-week-old mice with SRBC. Eight days following

266 immunization, we performed immunohistochemical (IHC) analysis on spleens with peanut agglutinin,

267 a GC marker. Staining revealed a significant decrease in overall number and size of GCs in

268 $Ubr5^{\Delta HECT/\Delta HECT}$ mice, but in white pulp with GCs, there were multiple small GCs (Figure 4C). Only

269 ~65% of white pulp in spleens of $Ubr5^{\Delta HECT/\Delta HECT}$ mice contained GCs compared to ~83% in WT

270 littermate controls. We evaluated the ability of follicular B cells to terminally differentiate into plasma

271 cells within PB and found a ~50% reduction of B cells and plasma cells (Figure 4D-E; Supplemental

272 Figure 1G-H). Although we had a significant decrease in CD138$^+$ antibody producing cells, levels of

273 IgG1, IgG3, and IgA were not changed in unstimulated $Ubr5^{\Delta HECT/\Delta HECT}$ mice (Figure 4F), and

274 measurement of antibodies IgG, IgM, and IgA within sera were unaltered suggesting that $Ubr5$ HECT

275 domain deletion does not affect basal antibody levels (Figure 4G). These studies indicate an important

276 role of Ubr5 in the function and activation of mature B cells.

277

278 **Loss of UBR5 HECT domain leads to increased expression of spliceosome components found**

279 **to interact with UBR5**

280   The HECT domain of UBR5 is thought to be required for its ubiquitination activity implicating

281 deletion could lead to increased accumulation of UBR5 substrates targeted for degradation by the

282 proteasome. To quantitatively determine protein differences in $Ubr5^{\Delta HECT/\Delta HECT}$ versus WT littermates,

283 we labeled splenic B220$^+$ cells with tandem mass tags (TMT), combined samples in equal

284   concentrations, and analyzed by MS (Figure 5A). Proteomic analysis identified 15,584 unique

285   peptides, 2,797 quantifiable proteins, and 1,675 proteins with greater than or equal to three unique

286   peptides. We identified 143 proteins that were either significantly decreased or enriched in

287   *Ubr5^ΔHECT/ΔHECT* B220⁺ splenocytes (Figure 5B and Supplementary Table 2). Principle component

288   analysis (PCA) plot showed protein isolated from 3 independent mice from either genotype clustered

289   together, but that the two independent genotypes clustered separately (Figure 5C). In addition,

290   identified proteins were distributed in different cellular compartments (Figure 5D). Of the differentially

291   expressed proteins, 104 ≥1.3 fold significantly overexpressed proteins were enriched for proteins

292   associated with mRNA processing, RNA splicing, and mRNA splicing via the spliceosome, whereas

293   the 39 ≤0.70 fold significantly decreased proteins in spleen B220⁺ cells from *Ubr5^ΔHECT/ΔHECT* were

294   proteins associated with immune system process and protein transport (Figure 5E-G). As suggested

295   by flowcytometry, IgD protein was the highest down-regulated protein following deletion of *Ubr5* HECT

296   domain (Figure 5E). CD22, which is associated with B cell activation, was also down-regulated in

297   correlation with the follicular B cell phenotype in *Ubr5^ΔHECT/ΔHECT* mice (Figure 5E). Intriguingly, the

298   second highest expressed protein in splenic B cells of *Ubr5^ΔHECT/ΔHECT* was UBR5 (Figure 5E-F).

299   Proteomic profiling revealed an increase in proteins associated with mRNA splicing in B cells lacking

300   HECT domain of UBR5 suggesting a novel role of UBR5 in mRNA splicing.

301

302   To identify putative substrates and interacting partners of UBR5 in MCL, we performed

303   immunoprecipitation followed by mass spectrometry (IP-MS) utilizing human MCL patient derived cell

304   lines, Jeko1 and Mino (Figure 6A).[24, 25] We identified 115 proteins with ≥3 unique peptides and, similar

305   to our TMT analysis, gene ontology analysis showed proteins enriched in mRNA splicing via the

306   spliceosome (Figure 6B and Supplementary Table 3). Comparing MS datasets from TMT labeled

13

307 proteins and endogenous IP-MS revealed 89 proteins overlapping and seven proteins were up-

308 regulated in the TMT study including UBR5 (Figure 7 D-E). Intriguingly, all six of the other identified

309 proteins are associated with mRNA splicing (SF3B3, SMC2, PRPF8, DHX15, SNRNP200, and

310 EFTUD2). These proteins are classified as core spliceosome components including U2 (SF3B3) and

311 associated U5 small nuclear ribonucleoprotein (snRNP) complex (EFTUD2, SNRNP200, and PRPF8)

312 (Figure 6E). Of the identified proteins, none have previously been characterized as UBR5 interactors

313 or substrates, suggesting a novel pathway of UBR5 regulation and the identification of potential novel

314 UBR5 substrates.

315

316 **Alterations in splicing factors and splicing in B cells.**

317   UBR5 has been implicated in a number of cellular processes including cell cycle (CDK9), DNA

318 damage (RNF168), and cell division (BUB3).[5-7, 26] BUB3 was found in the quantitative MS analysis;

319 however, accumulation was not seen in cells with deletion of *Ubr5* HECT domain (Supplementary

320 Table 1). In addition, western blot confirmed that BUB3, CDK9, and RNF-168 did not accumulate in

321 *Ubr5*$^{\Delta HECT/\Delta HECT}$ B220$^+$ splenocytes (Figure 7A). Flowcytometry validated cell surface markers

322 associated with activation and maturation, CD22 and IgD, expression was significantly decreased in

323 total B220$^+$ splenocytes (Figure 7B-C). UBR5 was the second highest expressed protein in the MS;

324 however, none of the identified peptides had coverage within the HECT domain (data not shown). To

325 confirm overexpression of UBR5 protein, we performed IHC and western blot analysis and found

326 higher protein expression of UBR5 in *Ubr5*$^{\Delta HECT/\Delta HECT}$ spleens (Figure 7A and D). In order to determine

327 if loss of HECT domain leads to stabilization of the protein, we performed half-life analysis with

328 cycloheximide treatment. *Ubr5*$^{\Delta HECT/\Delta HECT}$ B220$^+$ splenocytes had higher protein expression due to

329 stabilization of the protein (Figure 7E). These studies validate the MS findings that known substrates

330 do not accumulate and loss of the HECT domain leads to overexpression and stabilization of UBR5.

331

332 To evaluate protein overexpression of RNA splicing components, we performed western blot

333 analysis on B220$^+$ splenocytes. $Ubr5^{\Delta HECT/\Delta HECT}$ B220$^+$ splenocytes had increased expression of

334 EFTUD2, SMC2, and PRPF8 (Figure 7F). Because three of the identified proteins EFTUD2,

335 SNRNP200, and PRPF8 are part of the U5 snRNP complex, we wanted to determine whether UBR5

336 elutes with the U5 complex. We performed glycerol density gradient and found that EFTUD2,

337 SNRNP200, PRPF8, and UBR5 eluted in fractions 15-19 suggesting they are found in the same

338 complex (Figure 7G).

339

340 Expression of *IgM* and *IgD* is regulated by alternative splicing of the Ig heavy chain locus. As

341 shown in the follicular B cell population, *IgM* and *IgD* have aberrant expression suggesting defects in

342 splicing. To confirm altered splicing, we isolated follicular B cells from $Ubr5^{\Delta HECT/\Delta HECT}$ and WT

343 littermates for analysis of transcript levels. PCR confirmed increased *IgM* transcripts and decreased

344 *IgD* transcripts in $Ubr5^{\Delta HECT/\Delta HECT}$ follicular B cells (Figure 7H). It was previously shown that mRNA of

345 Zinc Finger Protein 318 (*Zfp318*) has two known splice variants.[27] It is thought that the longer

346 transcript form containing exon 1-10 plays a key role in alternative splicing of immunoglobulin heavy

347 chain locus. We found decreased expression of transcript spliced from exon 7 to exon 11 and aberrant

348 variant transcripts in $Ubr5^{\Delta HECT/\Delta HECT}$ follicular B cells, and decreased transcript containing exon 7 to

349 exon 9 suggesting expression of *Zfp318* splice variants may also be contributing to B cell defects

350 (Figure 7H). These studies demonstrate that loss of HECT domain leads to increased expression of

351 spliceosome components and aberrant splicing.

352

DISCUSSION

354

355   In this report, we demonstrate that ubiquitin E3 ligase UBR5 plays a key role in B cell

356   maturation and activation via regulation of alternative splicing. While UBR5 is present in all B

357   cell populations, deletion of *Ubr5* HECT domain had limited identifiable impact on development

358   of BM B cell populations. This suggests a crucial role for UBR5 in maturation of B cells. With

359   the loss of the UBR5 HECT domain, there is normal frequency of transitional B cells that

360   migrate to the spleen; although there is a block in differentiation of naïve B cells which

361   corresponds to the MCL tumor population. The greatest impact is on B1a and marginal zone

362   B cells that are significantly reduced within the spleen and peritoneal cavity suggesting

363   impaired innate immunity. Although follicular B cell population frequency is only slightly

364   impacted, these cells are phenotypically abnormal and have a reduced capacity to generate

365   plasma cells.

366

367   Interrogation of global proteomic changes in the splenic B cell population demonstrates a

368   novel role of UBR5 in mRNA splicing via the spliceosome. The spliceosome plays an important role

369   in providing genetic diversity. In immune cells, alternative splicing is suggested to play a key role in

370   B cell differentiation, activation, and survival.[28] A number of important pathways and genes in the

371   immune system require alternative splicing. In human B cells, ~90% of genes with multiple exons

372   undergo alternative splicing.[29] The spliceosome involves multicomponent complexes including five

373   snRNPs that coordinate mRNA splicing.[30] Our finding that components of the spliceosome are both

374   up-regulated and found interacting with UBR5 in MCL cell lines identifies a new pathway of UBR5

375   involvement. The striking phenotype of IgD in HECT domain mutants supports defects in splicing

376   since IgM and IgD are generated from alternative splicing of the heavy chain gene.[31] It is well

377   established that IgM and IgD play a key role in immunity and are required for B cell receptor

378   signaling and immune response, but little is known regarding how alternative splicing of *IgD* and

379   *IgM* occur. In addition, markers of mature naïve B cells, *CD21* and *CD23,* have multiple splice

380   variants regulated by alternative splicing.[32, 33] Our studies find that in transitional and follicular B

381   cell populations, *CD23* has altered expression, which may be due to splicing. Importantly,

382   expression of SF3B3 identified in our MS has been suggested to lead to alternative splicing of *Ezh2*

383   and promote tumorigenesis.[34] In addition, EZH2 has been previously shown to play a key role in

384   germinal center formation and EZH2 mutations promote lymphoid transformation.[35] Furthermore,

385   SF3B1, another component of the U2 snRNP complex that interacts with SF3B3 is frequently

386   mutated in chronic lymphoblastic leukemia and a variant of Myelodysplastic Syndrome, suggesting

387   that dysregulation of this complex may be important for development of hematopoietic

388   malignancies.[36, 37] Although these studies suggest a role of UBR5 in the spliceosome, further

389   investigation is required to determine if ubiquitination activity is required or whether UBR5 acts as

390   a scaffolding protein during splicing.

391

392   Loss of the HECT domain of UBR5 leads to stabilization and overexpression which could be

393   due to UBR5 potentially undergoing self-ubiquitination.[38] Also, UBR5 is predicted to bind RNA

394   further supporting its role in RNA splicing.[38] More importantly these studies identifying the

395   consequences of UBR5 HECT domain loss on alternative splicing in the immune system not only

396   reveal mechanisms regulating B cells development, but since ~18% of MCL patient genomes

397   contain UBR5 mutations, it may lead to further understanding of lymphoma transformation and

398   provide a potential therapeutic target. Overall, our findings reveal a novel mechanism of regulation

399   by UBR5 via alternative mRNA splicing, provides evidence that the ubiquitin E3 ligase is a novel

400   regulator of B cell maturation, and suggests a role of UBR5 in lymphoma transformation.

401

402 **AUTHOR CONTRIBUTIONS**

403 S.S., T.G, and S.M.B. conceived and designed the experiments. S.S., T.G., H.V., J.H.G, M.R.G.

404 and S.M.B preformed experiments and analysis. S.S., T.G., R.W.H., and S.M.B. wrote the

405 manuscript. H.C.H.L. and N.T.W. provided technical and material support. All authors reviewed the

406 manuscript before submission.

407

408

ACKNOWLEDGEMENTS

422

DISCLOSURES OF CONFLICTS OF INTEREST

424 The authors have no conflicts of interest related to this work.

425

426

REFERENCES

1. Vose, J.M. Mantle cell lymphoma: 2015 update on diagnosis, risk-stratification, and clinical management. *Am J Hematol* **90**, 739-745 (2015).

2. Schieber, M., Gordon, L.I. & Karmali, R. Current overview and treatment of mantle cell lymphoma. *F1000Res* **7** (2018).

3. Meissner, B. *et al.* The E3 ubiquitin ligase UBR5 is recurrently mutated in mantle cell lymphoma. *Blood* **121**, 3161-3164 (2013).

4. Morreale, F.E. & Walden, H. Types of Ubiquitin Ligases. *Cell* **165**, 248-248 e241 (2016).

5. Cojocaru, M. *et al.* Transcription factor IIS cooperates with the E3 ligase UBR5 to ubiquitinate the CDK9 subunit of the positive transcription elongation factor B. *J Biol Chem* **286**, 5012-5022 (2011).

6. Gudjonsson, T. *et al.* TRIP12 and UBR5 suppress spreading of chromatin ubiquitylation at damaged chromosomes. *Cell* **150**, 697-709 (2012).

7. Jiang, H., He, X., Feng, D., Zhu, X. & Zheng, Y. RanGTP aids anaphase entry through Ubr5-mediated protein turnover. *J Cell Biol* **211**, 7-18 (2015).

8. Jiang, W. *et al.* Acetylation regulates gluconeogenesis by promoting PEPCK1 degradation via recruiting the UBR5 ubiquitin ligase. *Mol Cell* **43**, 33-44 (2011).

9. Ong, S.S. *et al.* Stability of the human pregnane X receptor is regulated by E3 ligase UBR5 and serine/threonine kinase DYRK2. *Biochem J* **459**, 193-203 (2014).

10. Zhang, T., Cronshaw, J., Kanu, N., Snijders, A.P. & Behrens, A. UBR5-mediated ubiquitination of ATMIN is required for ionizing radiation-induced ATM signaling and function. *Proc Natl Acad Sci U S A* **111**, 12091-12096 (2014).

11. Liao, L. *et al.* E3 Ubiquitin Ligase UBR5 Drives the Growth and Metastasis of Triple-Negative Breast Cancer. *Cancer Res* **77**, 2090-2101 (2017).

12. Clancy, J.L. *et al.* EDD, the human orthologue of the hyperplastic discs tumour suppressor gene, is amplified and overexpressed in cancer. *Oncogene* **22**, 5070-5081 (2003).

13. Wang, J., Zhao, X., Jin, L., Wu, G. & Yang, Y. UBR5 Contributes to Colorectal Cancer Progression by Destabilizing the Tumor Suppressor ECRG4. *Dig Dis Sci* **62**, 2781-2789 (2017).

14. Zhang, Z. *et al.* Overexpression of UBR5 promotes tumor growth in gallbladder cancer via PTEN/PI3K/Akt signal pathway. *J Cell Biochem* (2019).

15. Quadros, R.M. *et al.* Easi-CRISPR: a robust method for one-step generation of mice carrying conditional and insertion alleles using long ssDNA donors and CRISPR ribonucleoproteins. *Genome Biol* **18**, 92 (2017).

16.   Huang, J. *et al.* RAD18 transmits DNA damage signalling to elicit homologous recombination repair. *Nature cell biology* **11**, 592-603 (2009).

17.   Strikoudis, A. *et al.* Regulation of transcriptional elongation in pluripotency and cell differentiation by the PHD-finger protein Phf5a. *Nature cell biology* **18**, 1127-1138 (2016).

18.   Man Chun John Ma, S.T., Alyssa Bouska, Tayla Heavican, Haopeng Yang, Qing Deng, Dalia Moore, Ariz Akhter, Keenan Hartert, Neeraj Jain, Jordan Showell, Sreejoyee Ghosh, Lesley Street, Marta Davidson, Christopher Carey, Joshua Tobin, Deepak Perumal, Julie M. Vose, Matthew A. Lunning, Aliyah R. Sohani, Benjamin J. Chen, Shannon Buckley, Loretta J. Nastoupil, R. Eric Davis, Jason R. Westin, Nathan H. Fowler, Samir Parekh, Maher Gandhi, Sattva Neelapu, Douglas Stewart, Javeed Iqbal, Scott J. Rodig, Adnan Mansoor, Michael R. Green Pathognomonic and epistatic genetic alterations in B-cell non-Hodgkin lymphoma . *bioRxiv* **674259** (2019).

19.   Saunders, D.N. *et al.* Edd, the murine hyperplastic disc gene, is essential for yolk sac vascularization and chorioallantoic fusion. *Mol Cell Biol* **24**, 7225-7234 (2004).

20.   Miura, H., Quadros, R.M., Gurumurthy, C.B. & Ohtsuka, M. Easi-CRISPR for creating knock-in and conditional knockout mouse models using long ssDNA donors. *Nat Protoc* **13**, 195-215 (2018).

21.   Lakso, M. *et al.* Efficient in vivo manipulation of mouse genomic sequences at the zygote stage. *Proc Natl Acad Sci U S A* **93**, 5860-5865 (1996).

22.   Hobeika, E. *et al.* Testing gene function early in the B cell lineage in mb1-cre mice. *Proc Natl Acad Sci U S A* **103**, 13789-13794 (2006).

23.   LeBien, T.W. & Tedder, T.F. B lymphocytes: how they develop and function. *Blood* **112**, 1570-1580 (2008).

24.   Jeon, H.J., Kim, C.W., Yoshino, T. & Akagi, T. Establishment and characterization of a mantle cell lymphoma cell line. *Br J Haematol* **102**, 1323-1326 (1998).

25.   Lai, R. *et al.* Establishment and characterization of a new mantle cell lymphoma cell line, Mino. *Leuk Res* **26**, 849-855 (2002).

26.   Scialpi, F., Mellis, D. & Ditzel, M. EDD, a ubiquitin-protein ligase of the N-end rule pathway, associates with spindle assembly checkpoint components and regulates the mitotic response to nocodazole. *J Biol Chem* **290**, 12585-12594 (2015).

27.   Ishizuka, M. *et al.* Molecular cloning and characteristics of a novel zinc finger protein and its splice variant whose transcripts are expressed during spermatogenesis. *Biochem Biophys Res Commun* **301**, 1079-1085 (2003).

28.   Yabas, M., Elliott, H. & Hoyne, G.F. The Role of Alternative Splicing in the Control of Immune Homeostasis and Cellular Differentiation. *Int J Mol Sci* **17** (2015).

29.   Toung, J.M., Morley, M., Li, M. & Cheung, V.G. RNA-sequence analysis of human B-cells. *Genome Res* **21**, 991-998 (2011).

499 30. Schaub, A. & Glasmacher, E. Splicing in immune cells-mechanistic insights and emerging
500   topics. *Int Immunol* **29**, 173-181 (2017).

501 31. Koop, B.F. *et al.* Analysis and comparison of the mouse and human immunoglobulin heavy
502   chain JH-Cmu-Cdelta locus. *Mol Phylogenet Evol* **5**, 33-49 (1996).

503 32. Illges, H., Braun, M., Peter, H.H. & Melchers, I. Analysis of the human CD21 transcription unit
504   reveals differential splicing of exon 11 in mature transcripts and excludes alternative splicing
505   as the mechanism causing solubilization of CD21. *Mol Immunol* **34**, 683-693 (1997).

506 33. Montagnac, G. *et al.* Differential role for CD23 splice forms in apical to basolateral transcytosis
507   of IgE/allergen complexes. *Traffic* **6**, 230-242 (2005).

508 34. Chen, K. *et al.* Alternative Splicing of EZH2 pre-mRNA by SF3B3 Contributes to the
509   Tumorigenic Potential of Renal Cancer. *Clin Cancer Res* **23**, 3428-3441 (2017).

510 35. Beguelin, W. *et al.* EZH2 is required for germinal center formation and somatic EZH2
511   mutations promote lymphoid transformation. *Cancer Cell* **23**, 677-692 (2013).

512 36. Lin, C.C. *et al.* SF3B1 mutations in patients with myelodysplastic syndromes: the mutation is
513   stable during disease evolution. *Am J Hematol* **89**, E109-115 (2014).

514 37. Wan, Y. & Wu, C.J. SF3B1 mutations in chronic lymphocytic leukemia. *Blood* **121**, 4627-4634
515   (2013).

516 38. Huibregtse, J.M., Scheffner, M., Beaudenon, S. & Howley, P.M. A family of proteins
517   structurally and functionally related to the E6-AP ubiquitin-protein ligase. *Proc Natl Acad Sci U
518   S A* **92**, 2563-2567 (1995).
519

520

521

522

523 **FIGURE LEGENDS**

524

525 **Figure 1. Expression of *Ubr5* in B cells and generation of conditional *Ubr5* HECT domain**

526 **knockout model. (**A) Frequency of UBR5 mutations in lymphoma patients. orange =

527 nonsense/frameshift; green = missense. (B) Relative qRT-PCR and (C) Western blot

528 expression of UBR5 within different B cell populations: pro B cells (B220$^+$IgM$^-$ckit$^+$), pre B cells

529 (B220$^+$IgM$^-$CD25$^+$), immature B cells (B220$^+$IgM^{lo}IgD$^-$) from the BM, and transitional

530 (B220$^+$CD93$^+$), marginal zone B cells (B220$^+$CD21$^+$CD23$^-$), and follicular B cells

531 (B220$^+$CD21$^+$CD23$^+$) isolated from the spleen of 6 weeks old WT C57Bl6 mice. (D) Schematic

532 of targeting strategy used to insert loxP sites flanking exon 58 of *Ubr5*. (E) Distribution of pups

533 born from crossing *Ubr5$^{ΔHECT/ΔHECT}$* with E2A^{CRE} (F) Pups alive at birth per genotype. (G)

534 Genotyping PCR of targeted alleles and deletion in six-week old mice bred to B lymphocyte

535 specific *Mb1^{Cre}* mouse model. PCR was performed on BM. (H) Relative expression of *Ubr5*

536 and *Ubr5* HECT domain by qRT-PCR in spleen B220$^+$ cells.

537

538 **Figure 2. The loss of the HECT domain of *Ubr5* leads to decreased numbers of mature**

539 **B cells within the BM.**

540 (A) Bar graph of the total number of cells per femur. (B) Representative flowcytometry plot of

541 total B220$^+$ in the BM. (C) Bar graph of the frequency of B220$^+$ cells per femur. (D)

542 Representative flowcytometry plots gated on B220$^+$ cells for pro and pre B cells (B220$^+$IgM$^-$

543 IgD$^-$), immature B cells (B220$^+$IgM^{lo}IgD$^-$), transitional B cells (B220$^+$IgM$^+$IgD$^-$), early mature B

544 cells (B220$^+$IgM$^+$IgD$^+$), and late mature B cells (B220$^+$IgM$^-$IgD$^+$). (E) Bar graphs of B cell

545 populations shown in D. (F) Representative flow cytometry plots gated for pro and pre B cells

24

546 (B220$^+$IgM$^-$), immature B cells (B220$^+$IgM^{lo}), and recirculating B cells (B220$^+$IgM$^+$). (G) Bar

547 graph of the population breakdown shown in F. (H) A representative flowcytometry plot gated

548 on B220$^+$ cells gating for pro B cells (B220$^+$IgM$^-$c-kit$^+$) and pre B cells (B220$^+$IgM$^-$CD25$^+$) (I)

549 Bar graph representing the population breakdown shown in H.

550 (N=10, * P<0.05, ** P<0.01, *** P<0.001)

551

552 **Figure 3. The loss of the HECT domain of *Ubr5* leads to reduction in marginal and B1a**

553 **splenic cells, but no effects on transitional B cells.**

554 (A) Bar graph of spleen weight. (N=19) (B) Bar graph of the total number of splenocytes. (N=4)

555 (C) Bar graph of frequency of B220$^+$ cells per spleen. (N=4) (D) An example hematoxylin and

556 eosin stain of spleens. (N=4) (E) Representative flow cytometry plot gated on B220$^+$ for

557 transitional cells: T1 cells (B220$^+$CD93$^+$IgM$^+$CD23$^-$), T2 cells (B220$^+$CD93$^+$IgM$^+$CD23$^+$), and

558 T3 cells (B220$^+$CD93$^+$IgM$^-$CD23$^+$). (N=5) (F-G) Bar graphs of percentages and absolute

559 number of transitional cells within the spleen. (H) Representative flowcytometry plots gated on

560 B220$^+$ for follicular B cells (B220$^+$CD21$^+$CD23$^+$) and marginal zone B cells (B220$^+$CD21$^+$CD23$^-$

561). (N=7) (I-J) Bar graphs of percentages and absolute number of follicular and marginal zone

562 B cells within the spleen. (K) Representative flowcytometry plots gated for B1a

563 (B220$^+$CD19^{lo}CD5$^+$) and B1b cells (B220$^+$CD19^{lo}CD5$^-$). (N=8) (L & M) Bar graph of

564 percentages and absolute number of B1a and B1b cells. (* P<0.05, ** P<0.01, *** P<0.001,

565 **** P<0.0001)

566

567 **Figure 4. The follicular B cells in *Ubr5*$^{\Delta HECT}$ mice have altered phenotype and diminished**

568 **differentiation capabilities.**

25

569 (A) Representative histogram of cell surface markers of $Ubr5^{WT}$ and $Ubr5^{\Delta HECT}$ follicular B cells

570 (B220$^+$CD21$^+$CD23$^+$). (B) Bar graphs of relative MFI of follicular B cells depicted in A. (C)

571 Representative PNA IHC staining of spleen 7 days post stimulation with SRBC. (D)

572 Representative flowcytometry plots of B220$^+$ and CD138$^+$ plasma cells in the peripheral blood.

573 (E) Bar graphs representing percentages of B220$^+$ and CD138$^+$ cells in the peripheral blood

574 depicted in D. (F) Bar graphs representing percentages of IgG1$^+$, IgG3$^+$, and IgA$^+$ B220$^+$ cells

575 in the peripheral blood. (G) Bar graphs of ELISA indicating relative expression for different

576 immunoglobulin types before (Day 0) and after (Day 8) immune system stimulation with SRBC.

577 (N=4) (* $P<0.05$, ** $P<0.01$, *** $P<0.001$, **** $P<0.0001$)

578

579 **Figure 5. Loss of HECT domain results in a reduction in B cell development proteins**

580 **and an enrichment in proteins regulating mRNA splicing. (**A) Schematic of sample

581 preparation of $UBR5^{WT}$ and $Ubr5^{\Delta HECT}$ spleens for TMT MS analysis. (N=3). (B) Quantification

582 of identified peptides and proteins. (C) PCA using components 1 and 2 showing clustering of

583 *WT* and *ΔHECT* samples for significantly up-regulated proteins. (D) Pie chart of localizations

584 for all 2,786 proteins identified by mass spec. (E) Volcano plot of the Log$_2$ fold change

585 *WT/ΔHECT* showing proteins significantly up-regulated (p<0.05) 1.3-fold or more and

586 significantly (p<0.05) down-regulated 0.7-fold or more. (F) Heatmap of the significantly up-

587 regulated and significantly down-regulated proteins showing the top 10 up-regulated and top

588 10 down-regulated proteins. (G) Gene ontology analysis showing pathways known to be

589 associated with significantly up-regulated ($\geq$1.3, p$\leq$0.05) and significantly down-regulated

590 ($\leq$0.7, p$\leq$0.05) proteins using DAVID 6.8 software. For up-regulated proteins, includes

26

591 pathways with ≥10 proteins associated and a p-value ≤0.01. Down-regulated proteins

592 pathways with p-value ≤0.05.

593

594 **Figure 6. UBR5 interacts with spliceosome components.** (A) Western blot of

595 immunoprecipitation of UBR5 from JEKO1 MCL cell line used for MS analysis. MS experiment

596 was performed in duplicate (B) Gene ontology analysis of immunoprecipitated proteins. (C)

597 Venn diagram showing the significant overlap of proteins identified in the TMT labelled $UBR5^{WT}$

598 and $Ubr5^{\Delta HECT}$ MS and those identified in the UBR5 endogenous IP MS. (D) Venn diagram

599 showing overlap of the proteins significantly up-regulated in the $Ubr5^{\Delta HECT}$ samples and those

600 identified in the UBR5 endogenous IP. (E) Spliceosome associated proteins found in

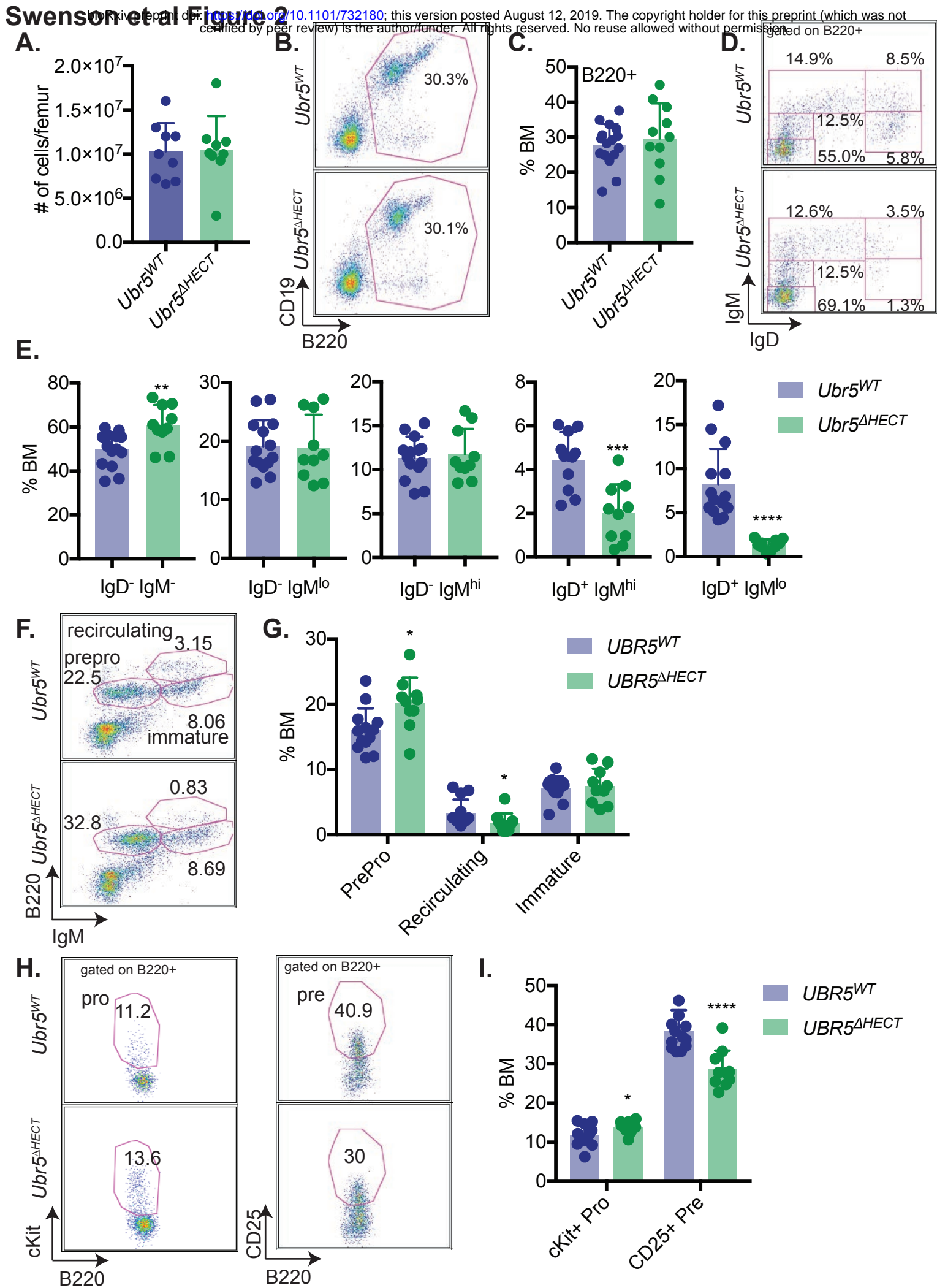601 endogenous immunoprecipitation and/or up-regulated in spleen B220+ cells.

602

603 **Figure 7. Loss of HECT domain leads to aberrant splicing.**

604 (A) Western blot of known UBR5 substrates in spleen B cells (B220+) $Ubr5^{WT}$ and $Ubr5^{\Delta HECT}$

605 mice. (B) Representative histogram of cell surface markers of spleen cells (B220+). (C) Bar

606 graphs of relative MFI of the markers in B. (D) Representative immunohistochemistry staining

607 of UBR5 protein in spleen. (E) Western blot of UBR5 in follicular B cells (B220+CD21+CD23+)

608 $Ubr5^{WT}$ and $Ubr5^{\Delta HECT}$ after treatment with 10µg/mL cycloheximide. (F) Western blot of proteins

609 identified in MS in spleenic B cells (B220+) $Ubr5^{WT}$ versus $Ubr5^{\Delta HECT}$ mice. (G) 10-30% glycerol

610 fractionation of nuclear lysate from HEK293T cells followed by western blot for UBR5 and

611 spliceosome components. (H) RT-PCR of mRNA in $Ubr5^{WT}$ and $Ubr5^{\Delta HECT}$ follicular B cells

612 (B220+CD21+CD23+). Arrows point to the bands of interest. (N=3) (** P<0.01, **** P<0.0001).
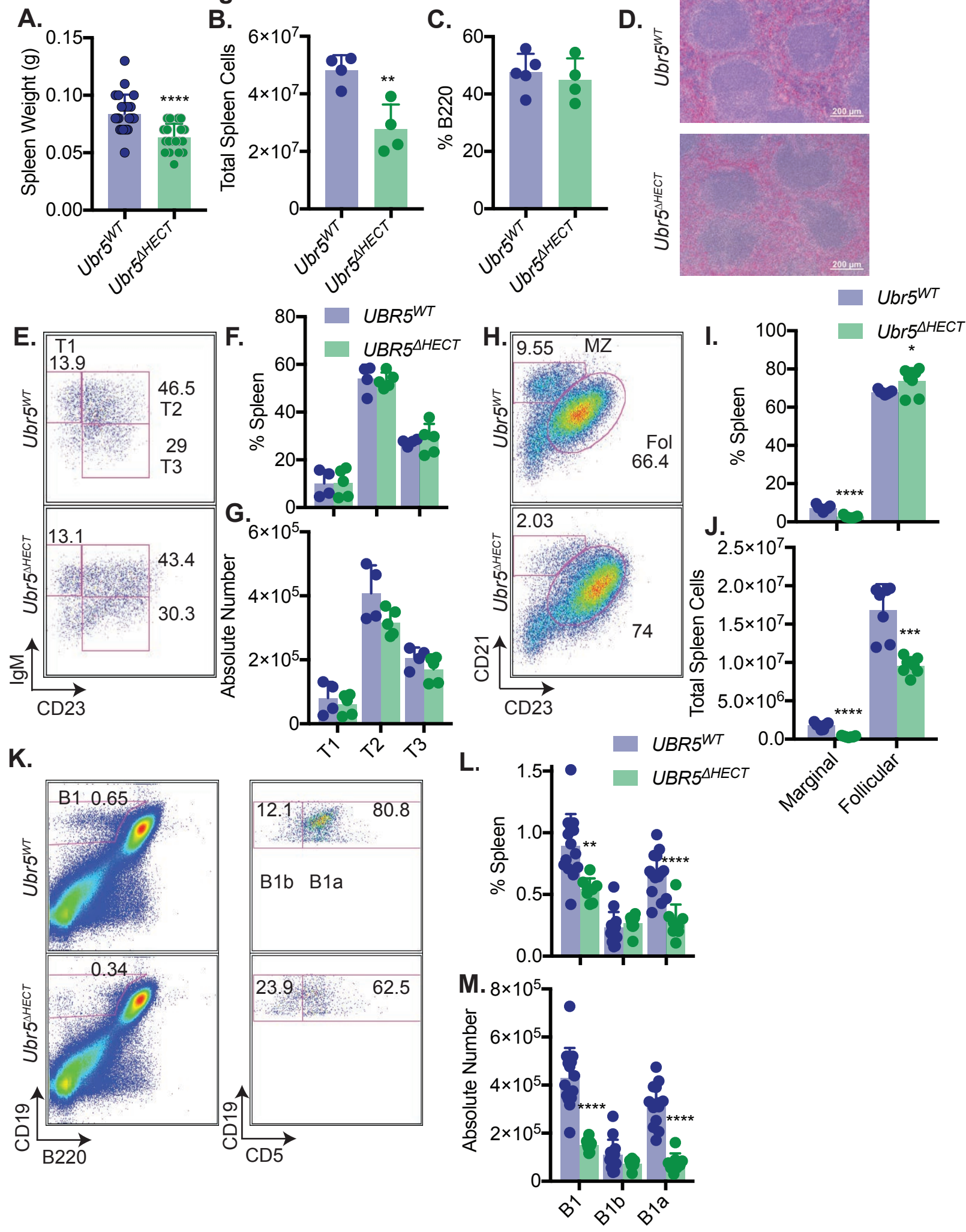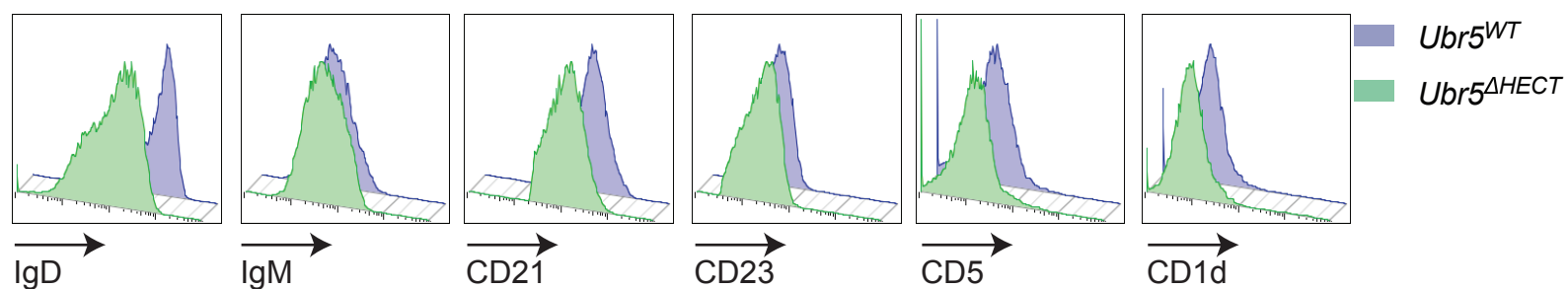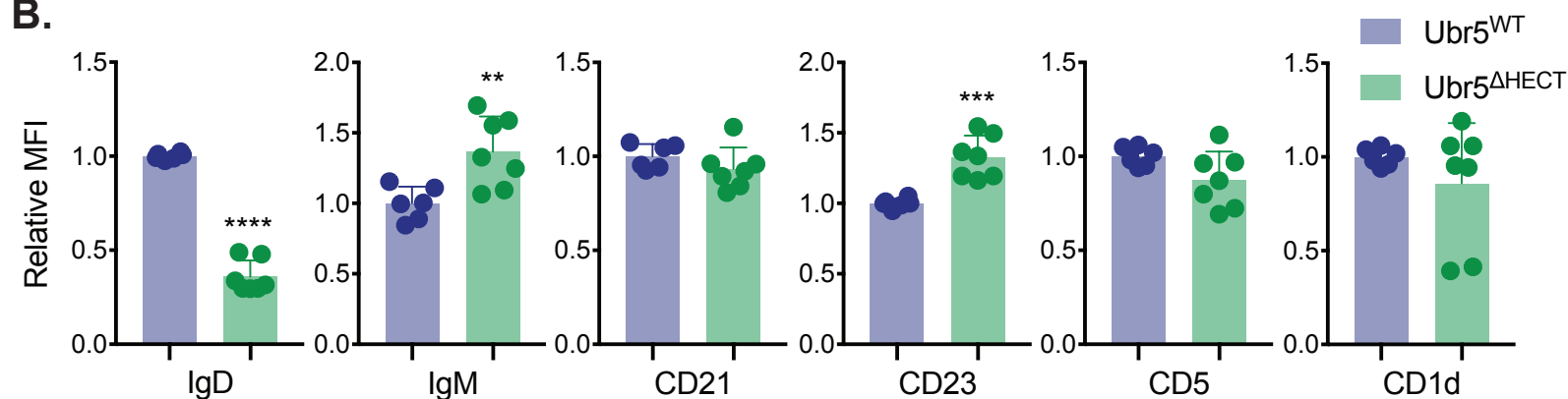
613

27

Swenson et al Figure 1
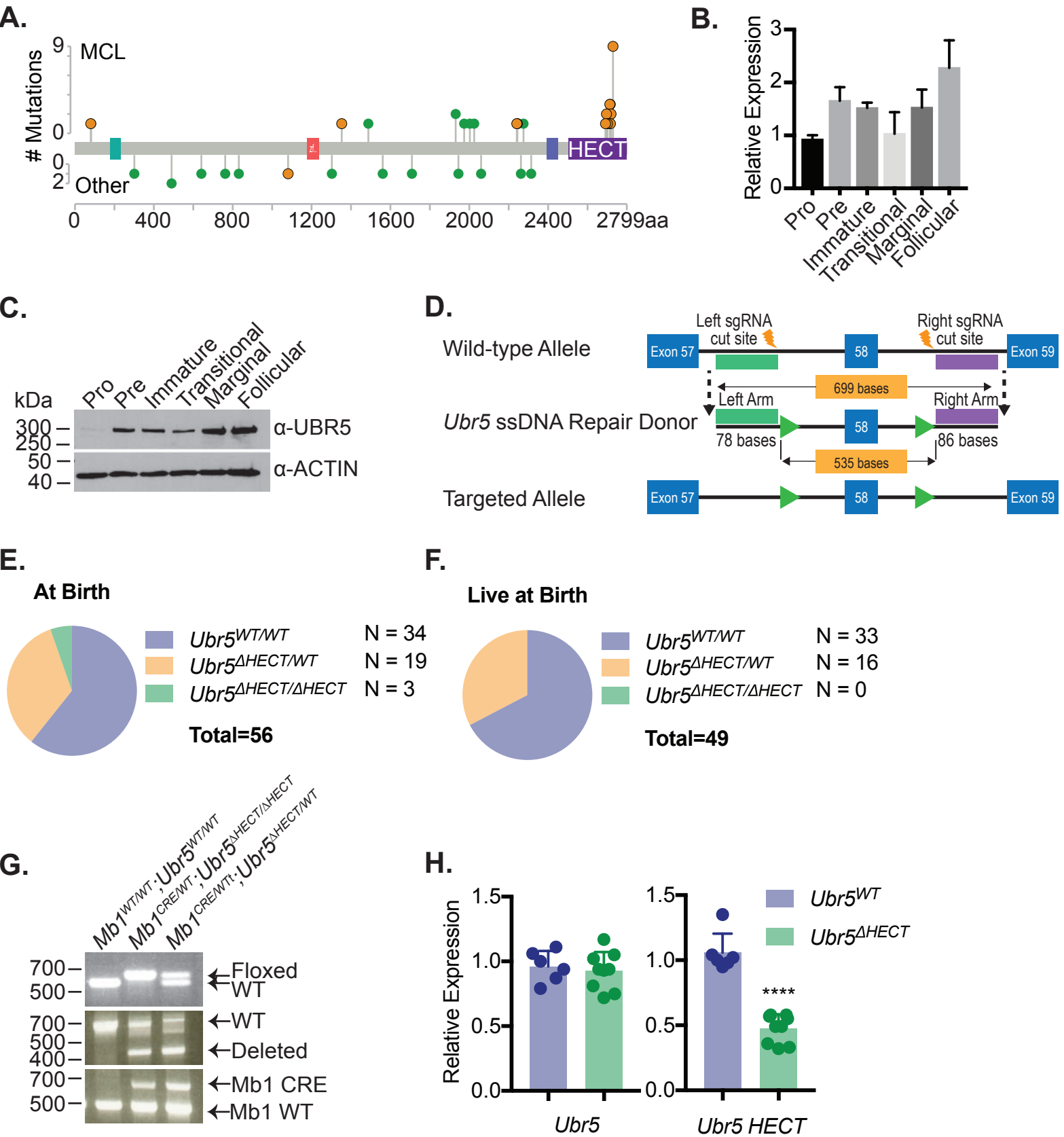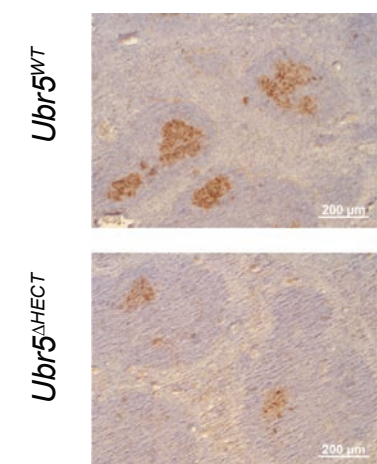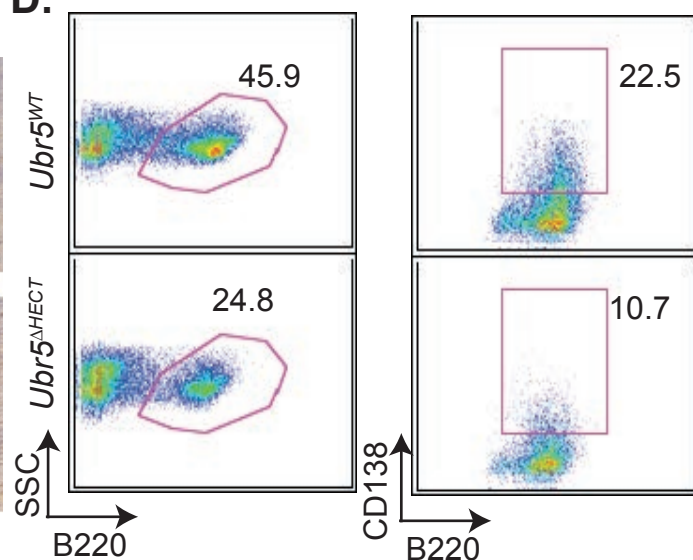
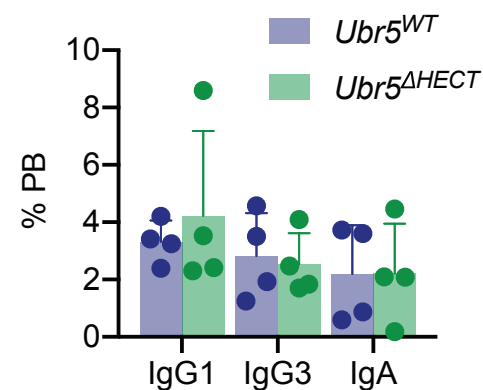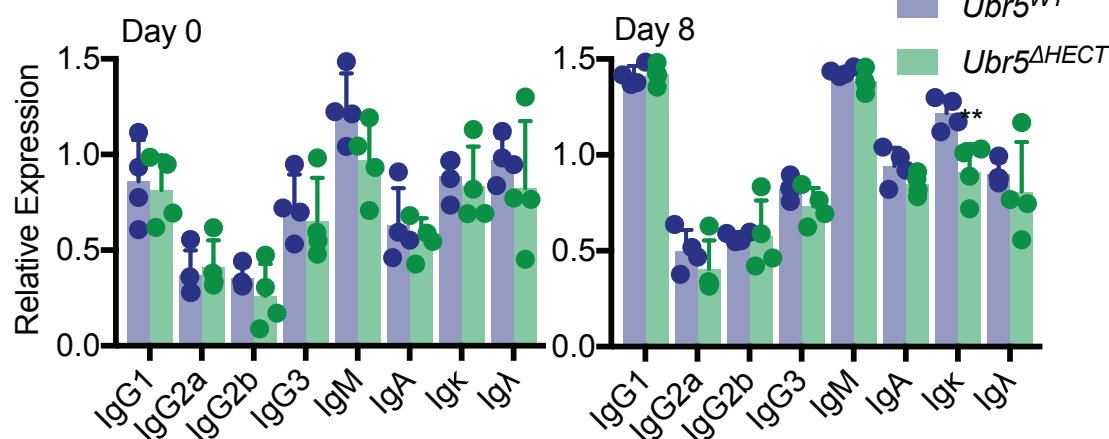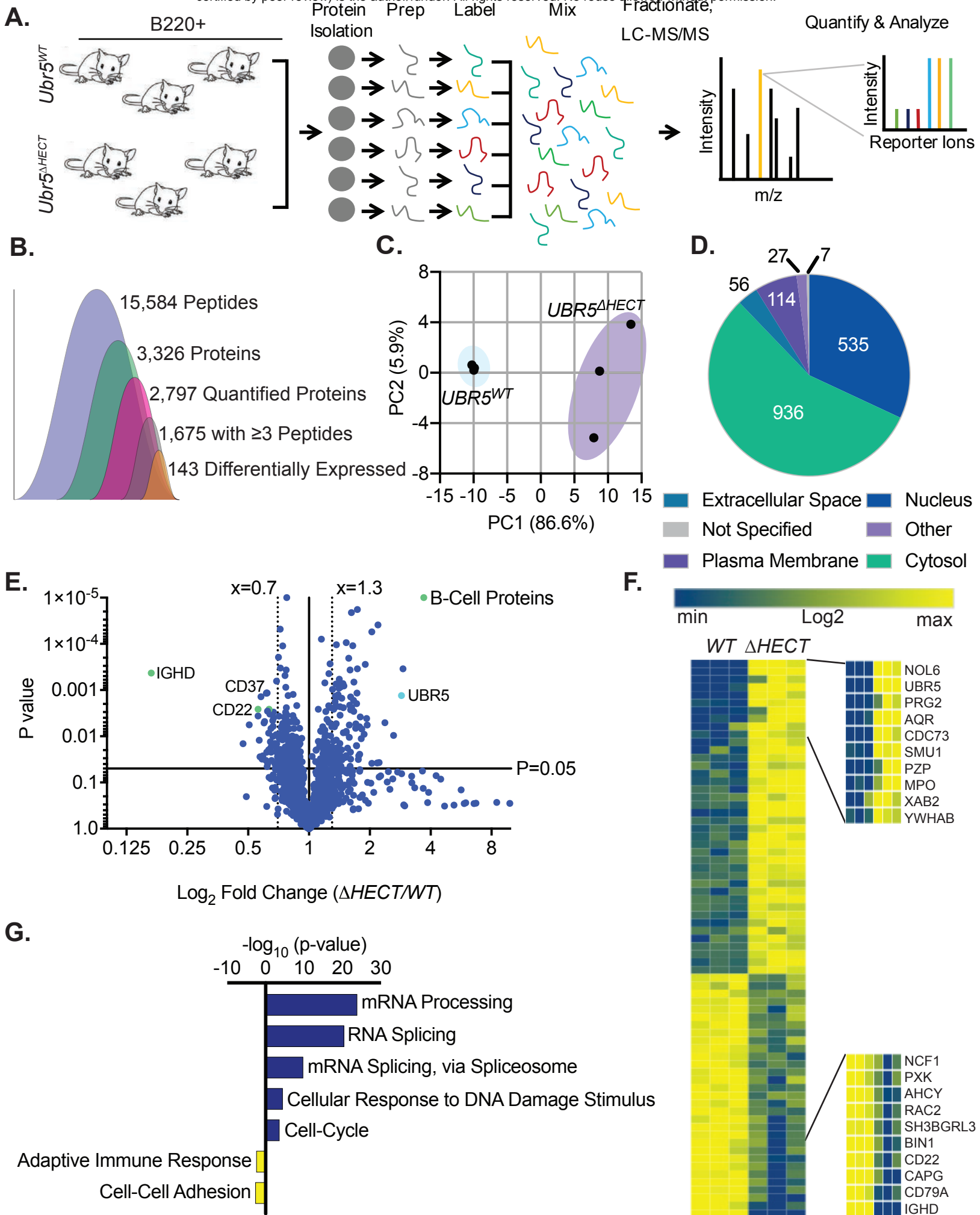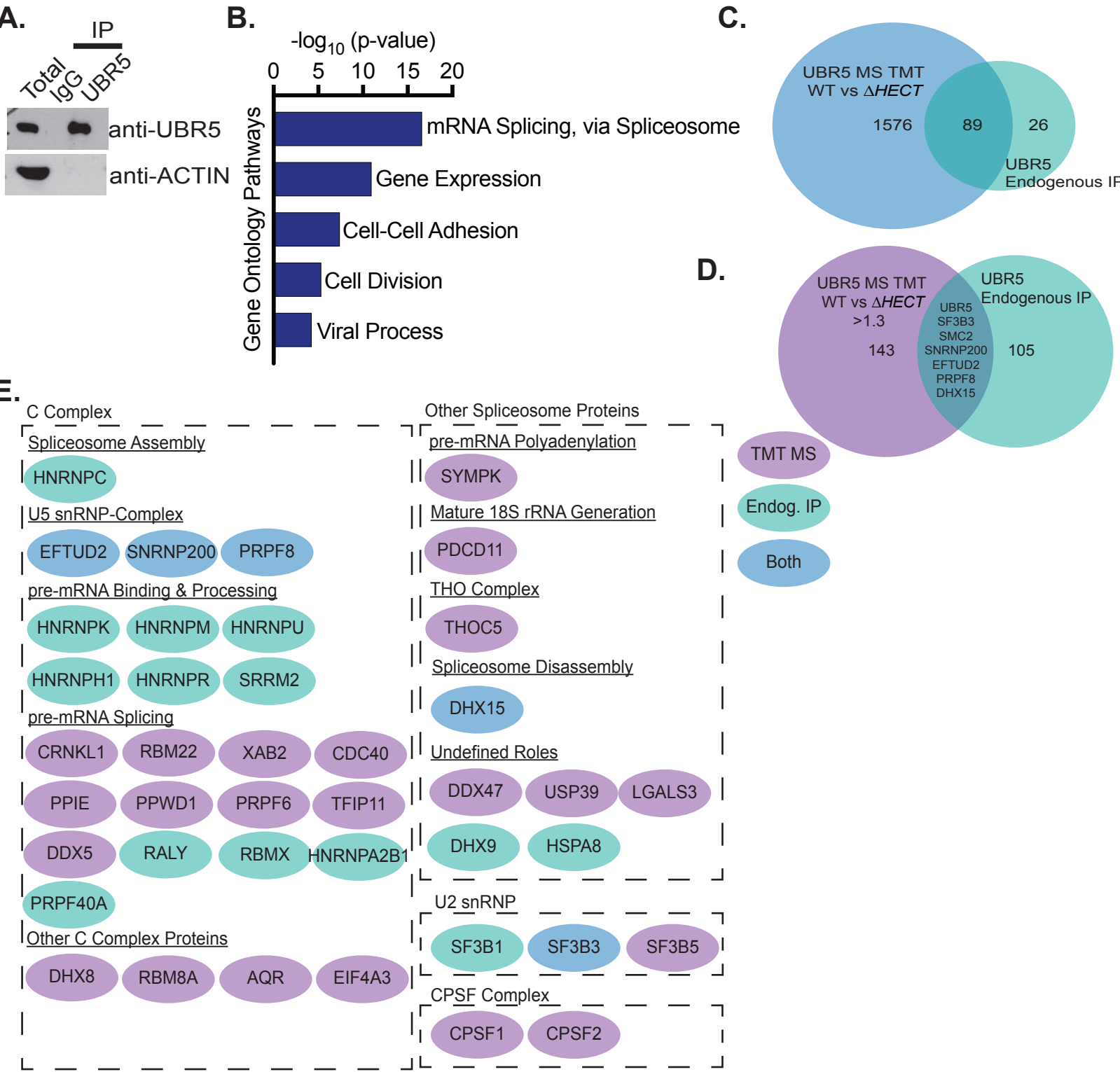# Swenson et al Figure 3

Swenson et al Figure 4

A.

B.

C.

D.

E.

F.

G.

Swenson et al Figure 6

A.

IP

Total IgG UBR5

anti-UBR5

anti-ACTIN

B.

-log₁₀ (p-value)

mRNA Splicing, via Spliceosome
Gene Expression
Cell-Cell Adhesion
Cell Division
Viral Process

Gene Ontology Pathways

C.

UBR5 MS TMT
WT vs ΔHECT
1576 89 26
UBR5
Endogenous IP

D.

UBR5 MS TMT
WT vs ΔHECT
>1.3
143

UBR5
Endogenous IP
UBR5
SF3B3
SMC2
SNRNP200
EFTUD2
PRPF8
DHX15
105

TMT MS
Endog. IP
Both

E.

C Complex

Spliceosome Assembly
HNRNPC

U5 snRNP-Complex
EFTUD2 SNRNP200 PRPF8

pre-mRNA Binding & Processing
HNRNPK HNRNPM HNRNPU
HNRNPH1 HNRNPR SRRM2

pre-mRNA Splicing
CRNKL1 RBM22 XAB2 CDC40
PPIE PPWD1 PRPF6 TFIP11
DDX5 RALY RBMX HNRNPA2B1
PRPF40A

Other C Complex Proteins
DHX8 RBM8A AQR EIF4A3

Other Spliceosome Proteins

pre-mRNA Polyadenylation
SYMPK

Mature 18S rRNA Generation
PDCD11

THO Complex
THOC5

Spliceosome Disassembly
DHX15

Undefined Roles
DDX47 USP39 LGALS3
DHX9 HSPA8

U2 snRNP
SF3B1 SF3B3 SF3B5

CPSF Complex
CPSF1 CPSF2

Swenson et al Figure 7